Supporting Information

Highly Active Pt_3Sn {110} Excavated Nanocube Cocatalysts for Photocatalytic Hydrogen Production

Juan Yao[1#], Yaru Zheng[1#], Xin Jia[2], Lixuan Duan[1], Qiang Wu[1]*, Cunping Huang[3], Wei An[2]*, Qunjie Xu[1, 4], Weifeng Yao[1, 4]*

[1]Shanghai Key Laboratory of Materials Protection and Advanced Materials in Electric Power, College of Environmental & Chemical Engineering, Shanghai University of Electric Power, Shanghai, P. R. China. [2]College of Chemistry and Chemical Engineering, Shanghai University of Engineering Science, Songjiang District, Shanghai 201620, P. R. China. [3]Aviation Fuels Research Laboratory, Federal Aviation Administration William J. Hughes Technical Center, Atlantic City International Airport, Atlantic City, NJ 08405, U.S.A.[4] Shanghai Institute of Pollution Control and Ecological Security, Shanghai, P. R. China.

***Corresponding Authors:** yaoweifeng@shiep.edu.cn and weian@sues.edu.cn and Qiangwu@shiep.edu.cn

#Juan Yao and Yaru Zheng contributed equally to this study and share first authorship

Experimental

Materials

Platinum (II) acetylacetonate ($Pt(acac)_2$) was purchased from Aladdin Industrial Corporation. Tin(Ⅱ) chloride dehydrate ($SnCl_2•2H_2O$) with purity greater than 98% was purchased from Sinopharm Chemical Reagent (Shanghai, China). Polyvinylpyrrolidone (PVP) was purchased from Shanghai Zhanyun Chemical Co., Ltd. Cadmium sulfide (CdS) was purchased from Sinopharm Chemical Reagent (Shanghai, China). Dimethylformamide (DMF) was purchased from Sinopharm Chemical Reagent (Shanghai, China). 5wt.% Nafion solution and sodium borohydride ($NaBH_4$) were purchased from Alfa Aesar. Tert-butylamine (TBA), acetone and ethanol solvents were obtained from Sinopharm Chemical Reagent Co. Ltd. All reagents used in this research were commercially available and used without further purification. Deionized water was obtained from an ULUPURE Ultra-pure water generator.

Preparation of Pt_3Sn/CdS and Pt/CdS photocatalysts

In a typical run, 2.5 mg prepared Pt_3Sn alloy nanoparticles were added into 100 mL deionized water containing 0.5000 g commercial CdS photocatalyst. The resulting suspension was stirred for 2 hours at room temperature. The mixture was then centrifuged at 8000 rpm for 3 minutes. Finally, the obtained powder was dried overnight in a vacuum oven at 333 K before grinding. It should be pointed out that PVP plays an important role in the synthesis of an excavated structure. However, PVP molecules strongly adsorbed onto the surface of Pt_3Sn and Pt nanoparticles are detrimental when the noble metal nanoparticles are used as cocatalysts. The complete removal of PVP from the Pt_3Sn/CdS and Pt/CdS was accomplished using the $NaBH_4$ and TBA treatments previously developed by our group.[1] The XRD pattern shows that the crystal structure of the Pt_3Sn/CdS composite are the same before and after the PVP removal process (Figure S1 of the Supporting Information).

2.3. Catalyst characterizations

Transmission electron microscopic (TEM) images and high-resolution transmission electron microscopic (HRTEM) images, together with selected area energy dispersive X-ray spectroscopy (EDS) were carried out using a field-emission transmission electron microscope (JEM-2100F) at

an accelerating voltage of 200 kV. The fluorescence spectrum was recorded with a fluorescence detector (FLS980, Edinburgh). Pt and Sn concentrations and alloy loadings were all determined by inductively coupled plasma atomic emission spectroscopy (ICP-AES Agilent 710). X-ray diffraction (XRD) patterns were collected on a BRUKER-D8 X-ray diffractometer using Cu Kα radiation. An ESCALAB250Xi spectrometer equipped with a monochromatized Al Kα (1486.6 eV) source was used for XPS analyses. Brunauer-Emmett-Teller (BET) specific surface areas were determined at 77 K on a Micrometrics Gemini VII 2390 surface area meter. UV-Vis absorption and diffusion reflectance spectra were recorded using a UV-Vis spectrometer (UV-2550, Shimadzu, Japan) and were then converted to absorption spectra based on the standard Kubelka–Munk method. $BaSO_4$ was used as a reflectance standard in the UV-Vis light diffuse reflectance experiments. All the electrochemical and photoelectrochemical measurements were performed in a typical three-electrode system using a CHI660E electrochemical station (CH Instruments, Inc., Shanghai).

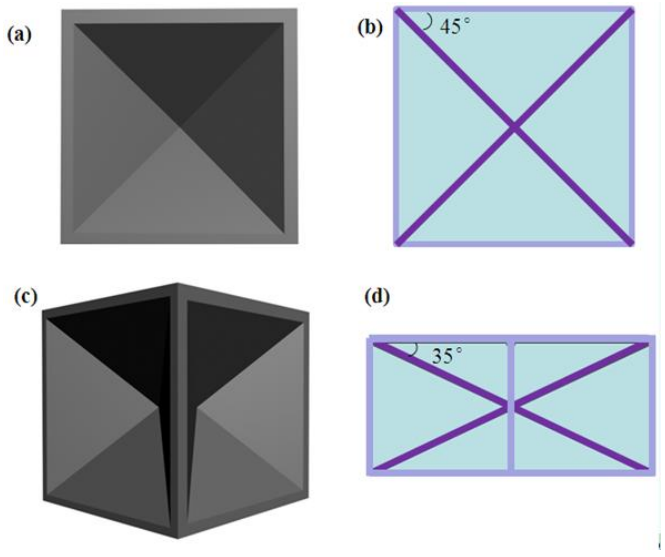

Scheme S1. Two schematic models of an excavated Pt_3Sn metal unit cell[2].

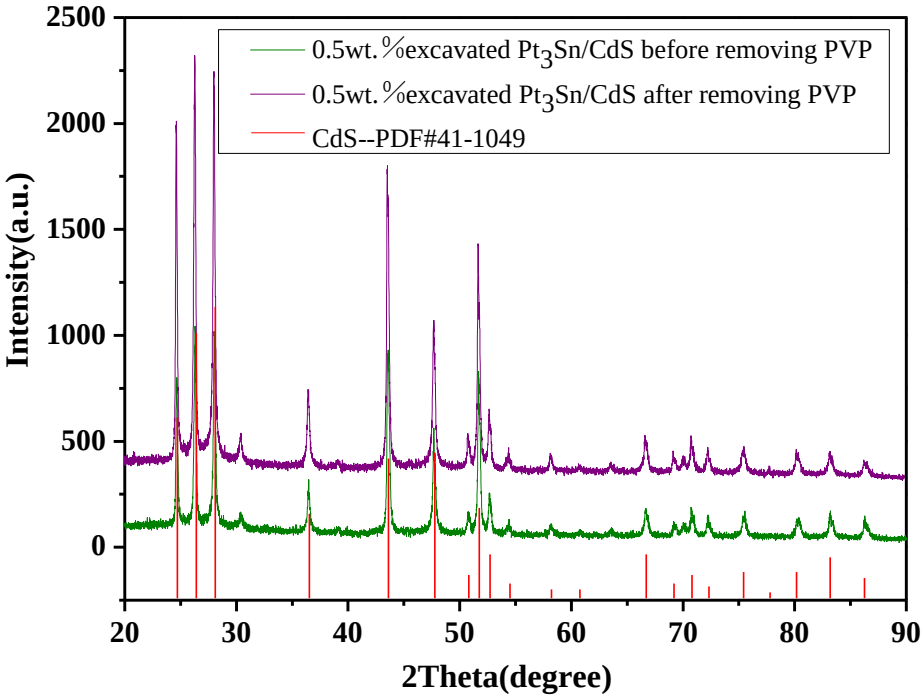

Figure S1. XRD patterns of 0.5 wt.% excavated Pt_3Sn nanocubes/CdS photocatalyst before and after PVP removal.

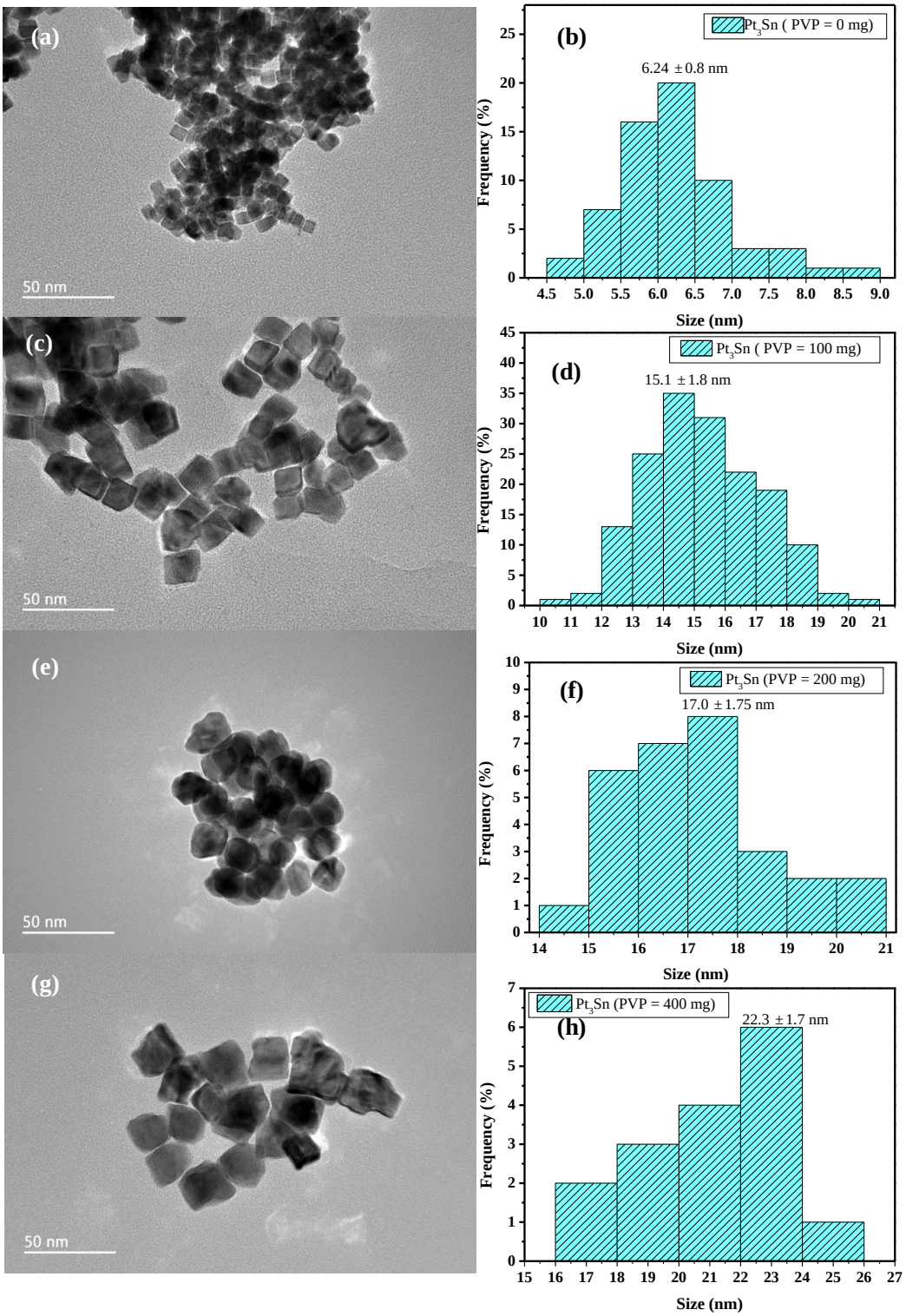

Figure S2. TEM images of Pt_3Sn alloy nanocubes synthesized at different PVP additions:(a) 0 mg, (c) 100 mg, (e) 200 mg, and (g) 400 mg and the corresponding particle size distribution histograms (b), (d), (f) and (h), respectively.

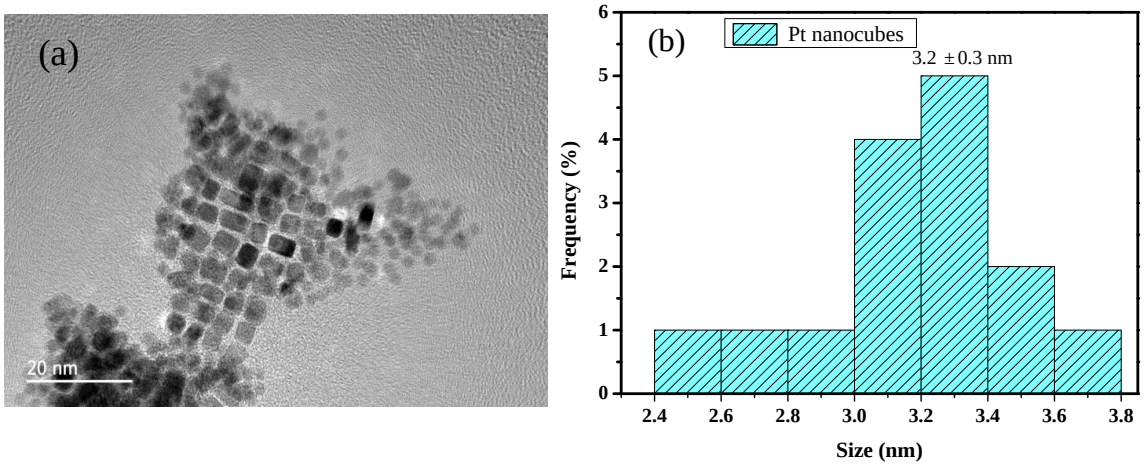

Figure S3. TEM image of Pt nanocubes (a) and particle size distribution histogram (b).

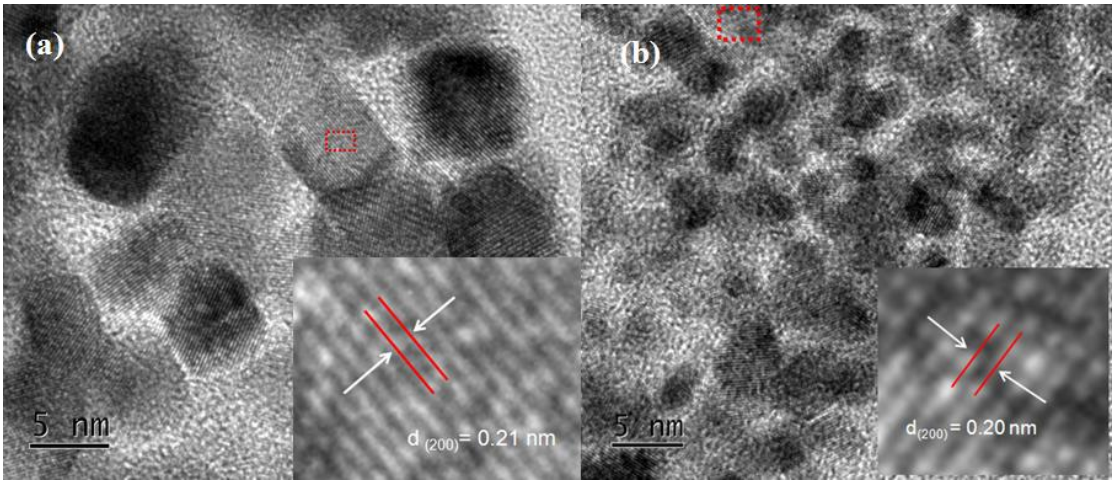

Figure S4. HRTEM images of Pt_3Sn nanocubes (a) and Pt nanocubes (b). (The insets are the fringes of Pt_3Sn and Pt crystal cells).

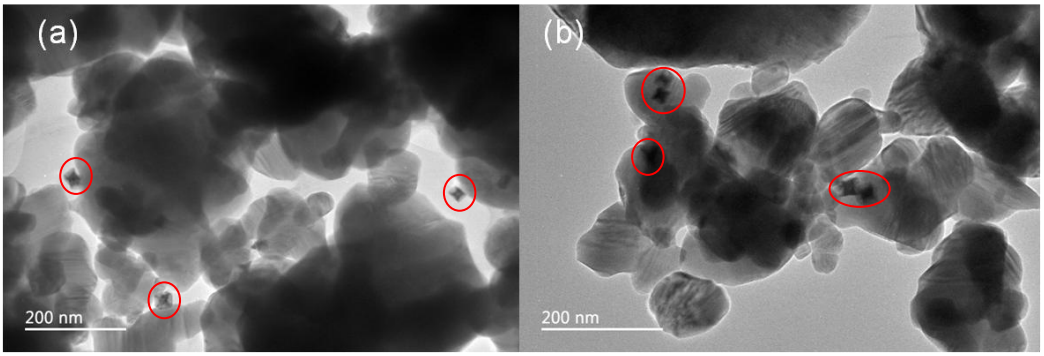

Figure S5. TEM images of 0.5 wt.% Pt_3Sn/CdS photocatalyst (a) before and (b) after photocatalytic hydrogen production. The highlighted particles are excavated Pt_3Sn nanocubes.

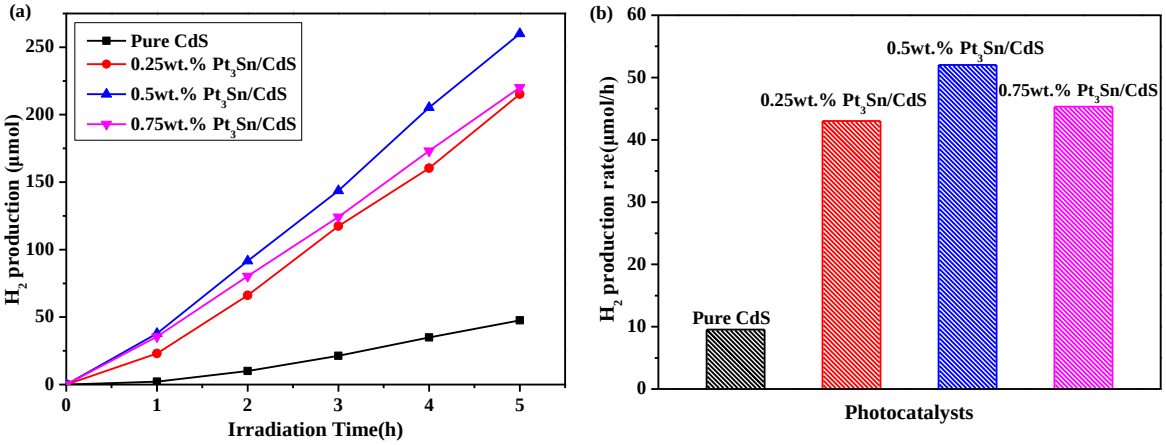

Figure S6. Hydrogen evolution (a) and hydrogen production rate histogram (b) for pure CdS, 0.25 wt.% excavated Pt_3Sn nanocubes/CdS, 0.5 wt.% excavated Pt_3Sn nanocubes/CdS and 0.75 wt.% excavated Pt_3Sn nanocubes/CdS. (Photocatalyst weight: 5.0 mg; Photolyte: 10 mL 1.25 M $(NH_4)_2SO_3$ solution; Photolyte pH: 8.4; Light source: 300 W Xe light with a cut-off filter ($\lambda > 420$ nm)).

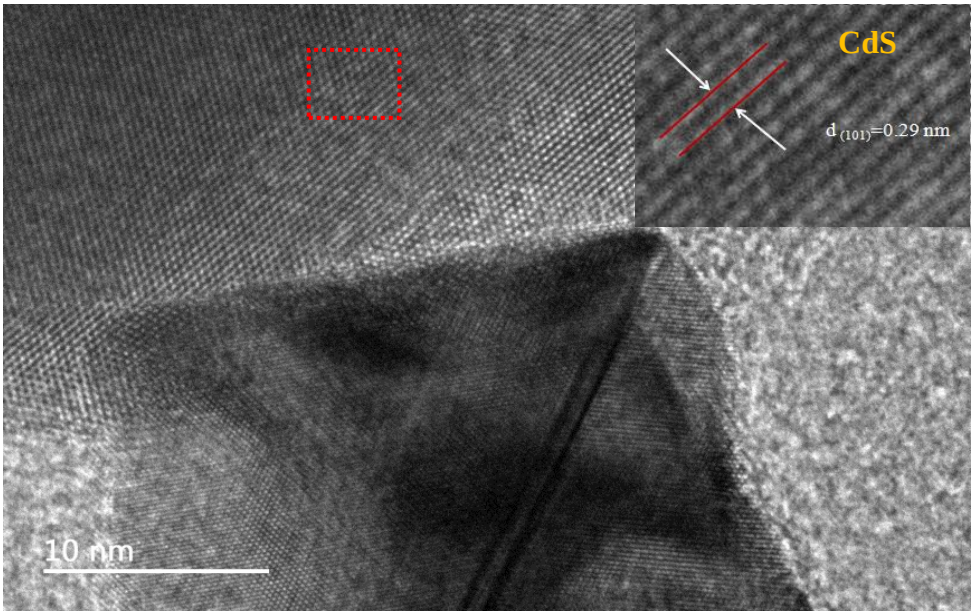

Figure S7. HRTEM images of an excavated Pt_3Sn nanocube loaded onto the surface of a CdS photocatalyst particle. The inset is the fringes of a CdS crystal.

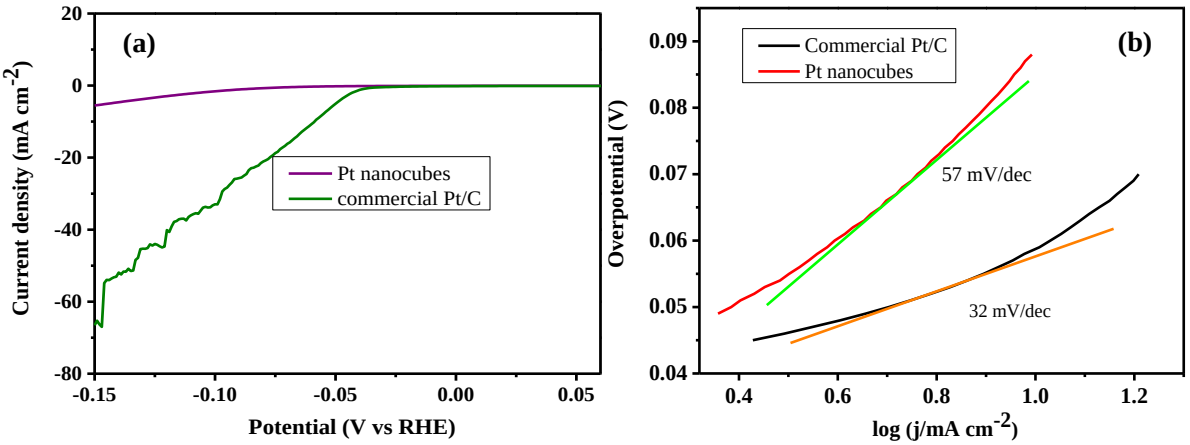

Figure S8. (a) Polarization curves of Pt nanocubes and commercial Pt/C at the same mass percent loading, (b) Tafel plot of commercial Pt/C.(Electrolyte: 0.5 M H_2SO_4, Scanning rate: 2 mV s^{-1})

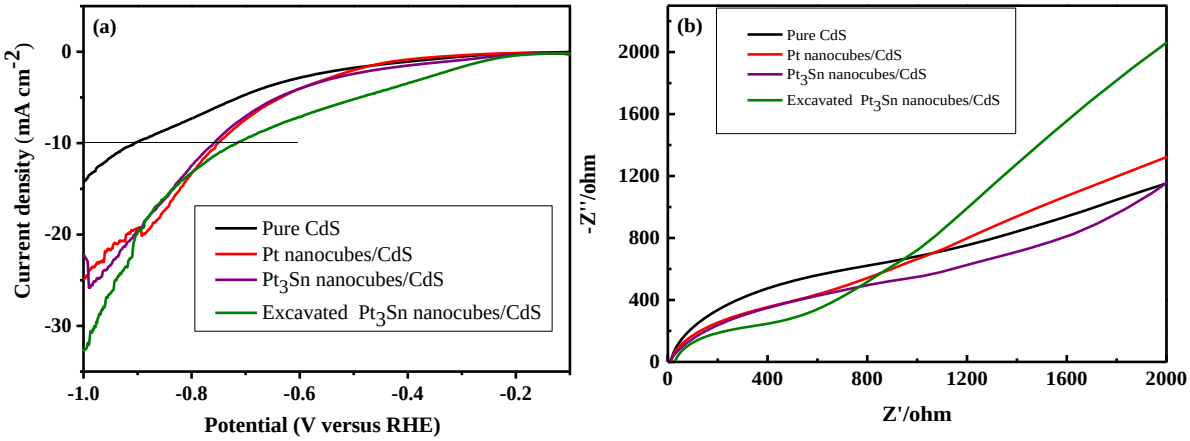

Figure S9. (a) Linear Scan Voltammetric (LSV) curves and (b) Electrochemical Impedance Spectra (EIS) for pure CdS, 0.5 wt.% Pt nanocubes/CdS , 0.5 wt.% Pt_3Sn nanocubes/CdS and 0.5 wt.% excavated Pt_3Sn nanocubes/CdS photocatalysts. (Electrolyte: 1.25 M $(NH_4)_2SO_3$ aqueous solution; Electrolyte pH = 8.4; Light Source: visible light irradiation (λ > 420 nm); Scanning rate: 2 mV s^{-1}; PVP addition: 300 mg).

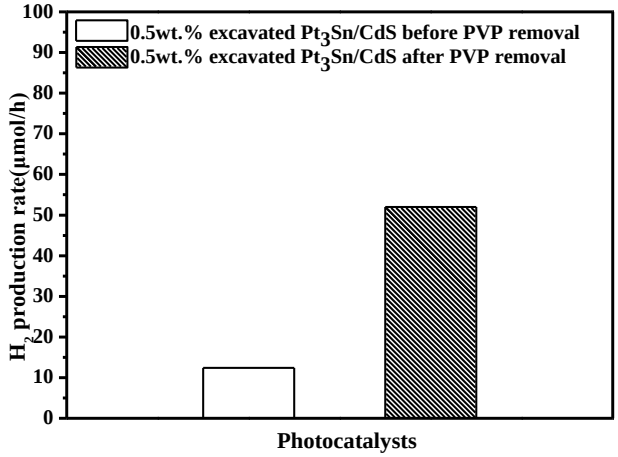

Figure S10. Hydrogen production rate histogram of 0.5 wt.% excavated Pt_3Sn nanocubes/CdS before and after PVP removal.

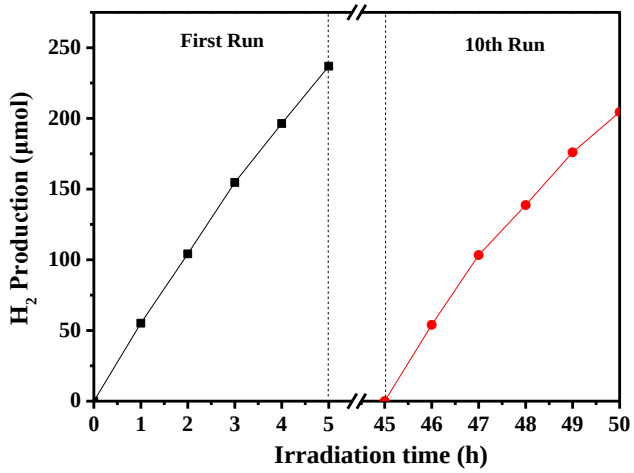

Figure S11. Cyclic lifespan tests for photocatalytic H_2 evolution via 0.5 wt.% excavated Pt_3Sn nanocubes/CdS photocatalyst.

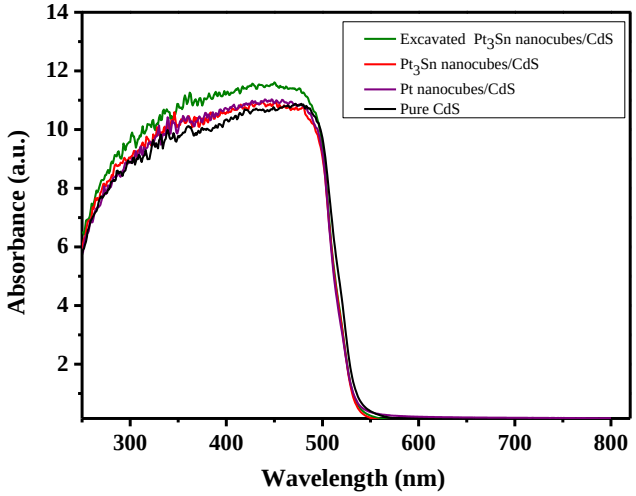

Figure S12. UV-Vis diffuse reflectance spectra (DRS) of pure CdS, 0.5 wt.% Pt nanocubes/CdS，0.5wt.% Pt_3Sn nanocubes/CdS and 0.5 wt.% excavated Pt_3Sn nanocubes/CdS.

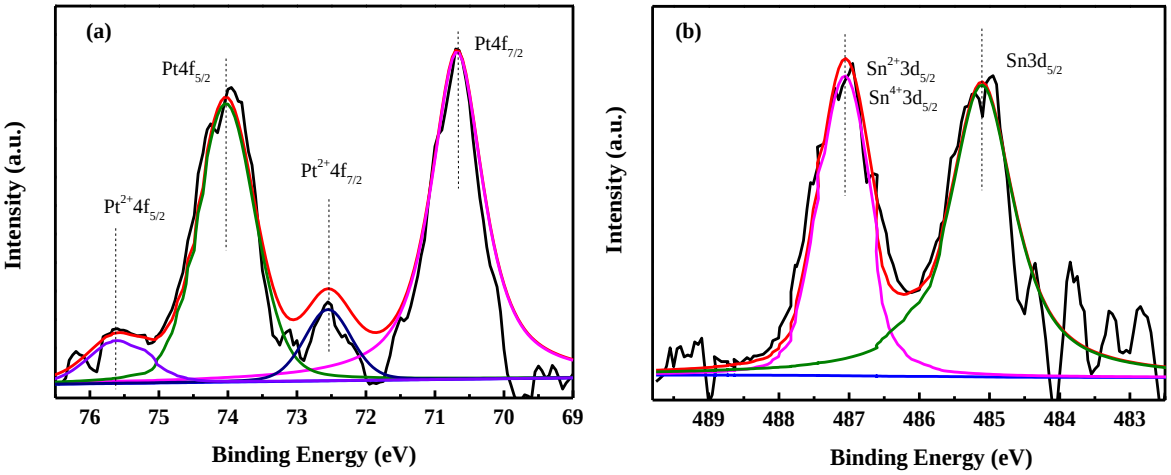

Figure S13. (a) Pt 4f and (b) Sn 3d XPS spectra of 0.5 wt.% excavated Pt_3Sn nanocubes.

Table S1. Hydrogen production rates and quantum efficiencies for three Pt and Pt_3Sn loaded CdS photocatalysts

Photocatalyst	H_2 production rate (μmol/h)	QE (at 420 nm) (%)
Bare CdS	9.8	16
0.5 wt. % Pt nanocubes/CdS (PVP = 300 mg)	15	25
0.5 wt. % Pt_3Sn nanocubes/CdS (PVP = 0 mg)	26	43
0.5 wt. % excavated Pt_3Sn nanocubes/CdS (PVP = 300 mg）	52	86

Table S2. BET specific surface areas for Pt and Pt_3Sn loaded CdS photocatalysts

Photocatalyst	BET (m^2/g)
Bare CdS	4.12
0.5 wt. % Pt nanocubes/CdS (PVP = 300 mg)	5.81
0.5 wt. % excavated Pt_3Sn nanocubes/CdS（PVP = 300 mg）	4.88

Table S3. Atomic ratios of Pt to Sn (Pt : Sn) in prepared Pt_3Sn alloy nanocubes based on energy dispersive X-ray spectroscopy (EDS) and inductively coupled plasma atomic emission spectroscopy (ICP) measurements

Photocatalyst	Pt:Sn (EDS)	Pt:Sn (ICP)
0.5 wt.% excavated Pt_3Sn nanocubes	77.1 : 22.9 (= 3.4)	77.5 : 22.5 (= 3.4)

Table S4. Summary of hydrogen production rates and quantum Efficiencies for CdS based photocatalysts

CdS based photocatalyst	Sacrificial Reagent	H_2 Production Rate	Quantum Efficiency	Ref.
WS_2-CdS(1-2 Layer)	lactic acid	17730 μmol $h^{-1}g^{-1}$	67% at 420 nm	Ref. [3]
4.0 wt.% WP/CdS	$(NH_4)_2SO_3$	155.17 μmol $h^{-1}g^{-1}$	10.2% at 420 nm	Ref.[4]
10 wt.% MoS_2/CdS	lactic acid	49800 μmol $h^{-1}g^{-1}$	41.37% at 420 nm	Ref.[5]
Pt/CdS	sulfite	3 μmol $h^{-1}g^{-1}$	9.6% at 455 nm	Ref.[6]
Pd-NCs/CdS	$(NH_4)_2SO_3$	814 μmol h^{-1}	-----	Ref.[7]
Pt-decorated CdSe@CdS	20 vol.% isopropyl alcohol	-----	27% at 455 nm	Ref.[8]
Pt−Pd/CdS	$(NH_4)_2SO_3$	1583 μmol·h^{-1}	54.0% at 420 nm	Ref.[9]
NiSx/CdS	lactic acid	2.86 mmol h^{-1}	60.4% at 420 nm	Ref.[10]
p-Au@CdS-TiO_2	Na_2S-Na_2SO_3	------	-----	Ref.[11]
4.2 wt% CdS/WS_2 /graphene	Na_2S-Na_2SO_3	1842 μmol $h^{-1}g^{-1}$	21.2% at 420 nm	Ref.[12]
Pt–PdS/CdS	Na_2S-Na_2SO_3	------	93% at 420 nm	Ref.[13]
0.5 wt.% Pt_3Sn/CdS	$(NH_4)_2SO_3$	24522.71μmol $h^{-1}g^{-1}$	86% at 420 nm	This work

Computational Details

The entropies of the gaseous molecules in this research were taken from the National Institute of Standards and Technology (NIST) Chemistry Webbook 6. The zero-point energy (ZPE) was calculated according to:

$$E_{ZPE} = \sum_{i=1}^{3N} \frac{h\nu_i}{2}$$

The entropy change for adsorbed intermediates was calculated within the harmonic approximation:

$$\Delta S_{ads}(0 \to T, P^0) = S_{vib} = \sum_{i=1}^{3N} \left[\frac{N_A h\nu_i}{T(e^{h\nu_i/k_B T} - 1)} - R\ln(1 - e^{-h\nu_i/k_B T}) \right]$$

Where: vi is DFT-calculated normal-mode frequency for species of 3N degrees of freedom (N = number of atoms that are adsorbed on Pt (100), Pt_3Sn (100), Pt (110) and Pt_3Sn (110) surfaces), N_A is the Avogadro's constant ($6.022 \times 1023\ mol^{-1}$), h is Planck's constant ($6.626 \times 10^{-34}\ J \cdot s$), k_B is the Boltzmann constant ($1.38 \times 10^{-23}\ J \cdot K^{-1}$), R is the ideal gas constant ($8.314\ J \cdot K^{-1}\ mol^{-1}$), and T is the system temperature (=298 °K in this work).

Table S5. Comparison of the calculated adsorption energies (in eV) of H* on Pt (100), Pt (110), Pt_3Sn (100), Pt_3Sn (110) facets

H adsorption Site	Pt (100)	Pt (110)	Pt_3Sn (100)	Pt_3Sn (110)
3F	–	-0.58 [T(Pt)]	–	**-0.29**
4F	-0.71[B][a]	–	-0.63[T(Pt)]	–
T(Pt)	-0.53	-0.58	**-0.63**	-0.28[3F]
T(Sn)	–	–	0.65	0.57
B(Pt-Pt)	**-0.71**	**-0.61**	–	0.70
B(Pt_3Sn)	–	–	-0.63[T(Pt)]	-0.28[3F]

[a] Sites in the brackets represent the final optimized adsorption sites.

Table S6. Lattice constants (a) of optimized Pt and Pt_3Sn unit cell and 2θ measured from simulated XRD compared with experimental XRD data.

	2θ(°)		Δ(2θ)(°)	
	Pt	Pt_3Sn	Calculated	Experimental
a (Å)	3.98	4.06	–	–
(111)	39.20	38.35	0.85	0.82
(200)	45.60	44.60	1.00	0.97
(220)	66.45	64.85	1.60	1.49
(311)	79.95	77.90	2.05	1.94
(222)	84.30	82.10	2.20	2.06

References:

(1) Luo, M.; Hong, Y.; Yao, W.; Huang, C.; Xu, Q.; Wu, Q. Facile Removal of Polyvinylpyrrolidone (PVP) Adsorbates from Pt Alloy Nanoparticles. *J. Mater. Chem. A* **2015,** *3* (6), 2770-2775.

(2) Chen, Q.; Yang, Y.; Cao, Z.; Kuang, Q.; Du, G.; Jiang, Y.; Xie, Z.; Zheng, L. Excavated Cubic Platinum-Tin Alloy Nanocrystals Constructed from Ultrathin Nanosheets with Enhanced Electrocatalytic Activity. *Agnew. Chem. Int. Ed.* **2016,** *55* (31), 9021-9025.

(3) Xu, D.; Xu, P.; Zhu, Y.; Peng, W.; Li, Y.; Zhang, G.; Zhang, F.; Mallouk, T. E.; Fan, X. High Yield Exfoliation of WS_2 Crystals into 1–2 Layer Semiconducting Nanosheets and Efficient Photocatalytic Hydrogen Evolution from WS_2/CdS Nanorod Composites. *ACS Appl. Mater. Interfaces* **2018,** *10, 2810-2818.*

(4) Zhang, J.; Yao, W.; Huang, C.; Shi, P.; Xu, Q. High Efficiency and Stable Tungsten Phosphide Cocatalysts for Photocatalytic Hydrogen Production. *J. Mater. Chem. A* **2017,** *5* (24), 12513-12519.

(5) Yin, X.L.; Li, L.L.; Jiang, W.J.; Zhang, Y.; Zhang, X.; Wan, L.J.; Hu, J.S. MoS_2/CdS Nanosheets-on-Nanorod Heterostructure for Highly Efficient Photocatalytic H_2 Generation under Visible Light Irradiation. *ACS Appl. Mater. Interfaces* **2016,** *8* (24), 15258-15266.

(6) Subbaraman, R.; Tripkovic, D.; Strmcnik, D.; Chang, K. C.; Uchimura, M.; Paulikas, A. P.; Stamenkovic, V.; Markovic, N. M. Enhancing Hydrogen Evolution Activity in Water Splitting by Tailoring Li^+-$Ni(OH)_2$-Pt Interfaces. *Science* **2011,** *334* (6060), 1256-1260.

(7) Luo, M.; Yao, W.; Huang, C.; Wu, Q.; Xu, Q. Shape-controlled Synthesis of Pd Nanoparticles for Effective Photocatalytic Hydrogen Production. *RSC Adv.* **2015,** *5* (51), 40892-40898.

(8) Nakibli, Y.; Kalisman, P.; Amirav, L. Less Is More: The Case of Metal Cocatalysts. *J. Phys. Chem. Lett.* **2015,** *6* (12), 2265-2268.

(9) Luo, M.; Lu, P.; Yao, W.; Huang, C.; Xu, Q.; Wu, Q.; Kuwahara, Y.; Yamashita, H. Shape and Composition Effects on Photocatalytic Hydrogen Production for Pt–Pd Alloy Cocatalysts. *ACS Appl. Mater. Interfaces* **2016,** *8* (32), 20667-20674.

(10) Qin, Z.; Chen, Y.; Wang, X.; Guo, X.; Guo, L. Intergrowth of Cocatalysts with Host Photocatalysts for Improved Solar-to-Hydrogen Conversion. *ACS Appl. Mater. Interfaces* **2016,** *8* (2), 1264-1272.

(11) Tong, R.; Liu, C.; Xu, Z.; Kuang, Q.; Xie, Z.; Zheng, L. Efficiently Enhancing Visible Light Photocatalytic Activity of Faceted TiO_2 Nanocrystals by Synergistic Effects of Core–Shell Structured Au@CdS Nanoparticles and Their Selective Deposition. *ACS Appl. Mater. Interfaces* **2016,** *8* (33), 21326-21333.

(12) Xiang, Q.; Cheng, F.; Lang, D. Hierarchical Layered WS_2/Graphene-Modified CdS Nanorods for Efficient Photocatalytic Hydrogen Evolution. *ChemSusChem* **2016,** *9* (9), 996-1002.

(13) Yang, J.; Yan, H.; Wang, X.; Wen, F.; Wang, Z.; Fan, D.; Shi, J.; Li, C. Roles of Cocatalysts in Pt–PdS/CdS with Exceptionally High Quantum Efficiency for Photocatalytic Hydrogen Production. *J.Catal.* **2012,** *290*, 151-157.